PERGAMON

Journal of Structural Geology 25 (2003) 1751–1771

JOURNAL OF STRUCTURAL GEOLOGY

www.elsevier.com/locate/jsg

Competent unit thickness variation in detachment folds in the Northeastern Brooks Range, Alaska: geometric analysis and a conceptual model

Paul K. Atkinson, Wesley K. Wallace*

Department of Geology & Geophysics and Geophysical Institute, University of Alaska Fairbanks, Fairbanks, AK 99775-5780, USA

Received 15 April 2001; received in revised form 12 December 2002; accepted 13 December 2002

Abstract

Detailed measurements of six map-scale detachment folds in the northeastern Brooks Range, Alaska, document significant variations in structural thickness of the competent Lisburne Limestone. Thickness variations occur mainly by parasitic folding and penetrative strain, and may be controlled by differences in mechanical stratigraphy, relative thicknesses of the competent and incompetent units, and structural relief of the underlying basement. The geometry of these detachment folds is not consistent with key assumptions of existing geometric and kinematic models, such as constant competent unit thickness or constant detachment depth. We propose a new model that allows both competent and incompetent unit thicknesses to vary throughout the fold. This model allows a more realistic geometric description of some natural detachment folds than previous models, but the number of variables makes unique reconstruction of specific fold geometries or kinematics difficult. Comparison of models with natural folds demonstrates that significant error can result if shortening estimates are based on models that incorrectly assume constant competent unit thickness or constant detachment depth. Use of surveying techniques to quantify map-scale fold geometry can provide better reconstructions of fold geometry, better shortening estimates, and information to constrain kinematic reconstructions.

Keywords: Detachment folds; Models; Geometry; Kinematics; Lisburne Limestone; Northeastern Brooks Range

1. Introduction

A detachment fold forms when a layer of rock deforms above a bedding-parallel thrust fault (also referred to as a detachment surface or décollement) (Jamison, 1987). Detachment folds are commonly found in mechanically layered stratigraphy, where a relatively competent unit (e.g. sandstone or limestone) overlies a relatively incompetent unit (e.g. salt or shale). Numerous examples have been described from fold-and-thrust belts throughout the world (e.g. Poblet and Hardy, 1995; Anastasio et al., 1997; Homza and Wallace, 1997; Fischer and Jackson, 1999).

Detachment folding plays an important role in thin-skinned deformation in fold-and-thrust belts worldwide, and must be accurately represented to correctly restore folded sections to their undeformed state. Understanding such structures also has important practical applications for hydrocarbon exploration and seismic hazard assessment. Despite its importance, detachment folding remains poorly understood. No published conceptual model adequately explains the wide variation in detachment fold geometries observed in the natural world, let alone how the folds evolved, either kinematically or mechanically. Existing models all impose very restrictive assumptions on the geometry and growth of a fold, thereby minimizing the variables and narrowing the range of possible outcomes. For example, most require parallel folding of the competent upper unit so that it maintains constant bed length and bed thickness (Dahlstrom, 1990; Homza and Wallace, 1997), or they restrict uniform thickness changes to the forelimbs of asymmetrical folds (Jamison, 1987; Poblet and McClay, 1996). To solve area balance problems, some models require fold limbs to lengthen by hinge migration (Dahlstrom, 1990; Poblet and McClay, 1996), or the structural thickness of the incompetent unit to vary (Homza and Wallace, 1997). Another model (Epard and Groshong, 1995) maintains area balance by allowing bed thickness to change systematically across the entire fold, which effectively assumes no

* Corresponding author. Fax: +907-474-5163.
E-mail address: wallace@gi.alaska.edu (W.K. Wallace).

0191-8141/03/$ - see front matter © 2003 Elsevier Science Ltd. All rights reserved.
PII: S0191-8141(03)00003-8

competency contrast between layers. But to what extent do these assumptions and requirements actually reflect reality? In particular, how does competent unit thickness vary across natural detachment folds?

Some of the world's best exposures of map-scale detachment folds are found in the Shublik and northern Franklin Mountains in the northeastern Brooks Range of Alaska (Fig. 1). These detachment folds have formed in the relatively competent Lisburne Limestone above a regional décollement in the thinner and less competent Kayak Shale (Fig. 2) (Wallace and Hanks, 1990; Wallace, 1993; Homza and Wallace, 1997). We analyzed the map-scale geometry of six of these folds in detail in order to document how the Lisburne Limestone responded to shortening by folding. Most importantly, we wanted to know how the Lisburne varies in structural thickness across these folds, how these thickness changes were accommodated, and what controlled these changes. We sought a better understanding of folding within the Lisburne to provide information to test various aspects of the published conceptual models, and ultimately to help define a more comprehensive and realistic model for the geometric and kinematic evolution of detachment folds. Insights from our analysis of detachment folds in the Lisburne should have broad applicability to comparable detachment folds worldwide.

This paper consists of two parts. The first documents our observations of the folds we studied. The second presents a conceptual model we developed to describe the thickness changes observed in the Lisburne Limestone, and compares this model both with the observed natural folds and with other published models.

2. A geometric analysis of detachment folds in the Shublik and northern Franklin Mountains

2.1. Geologic setting

2.1.1. Stratigraphy

The rocks that make up the Shublik and northern

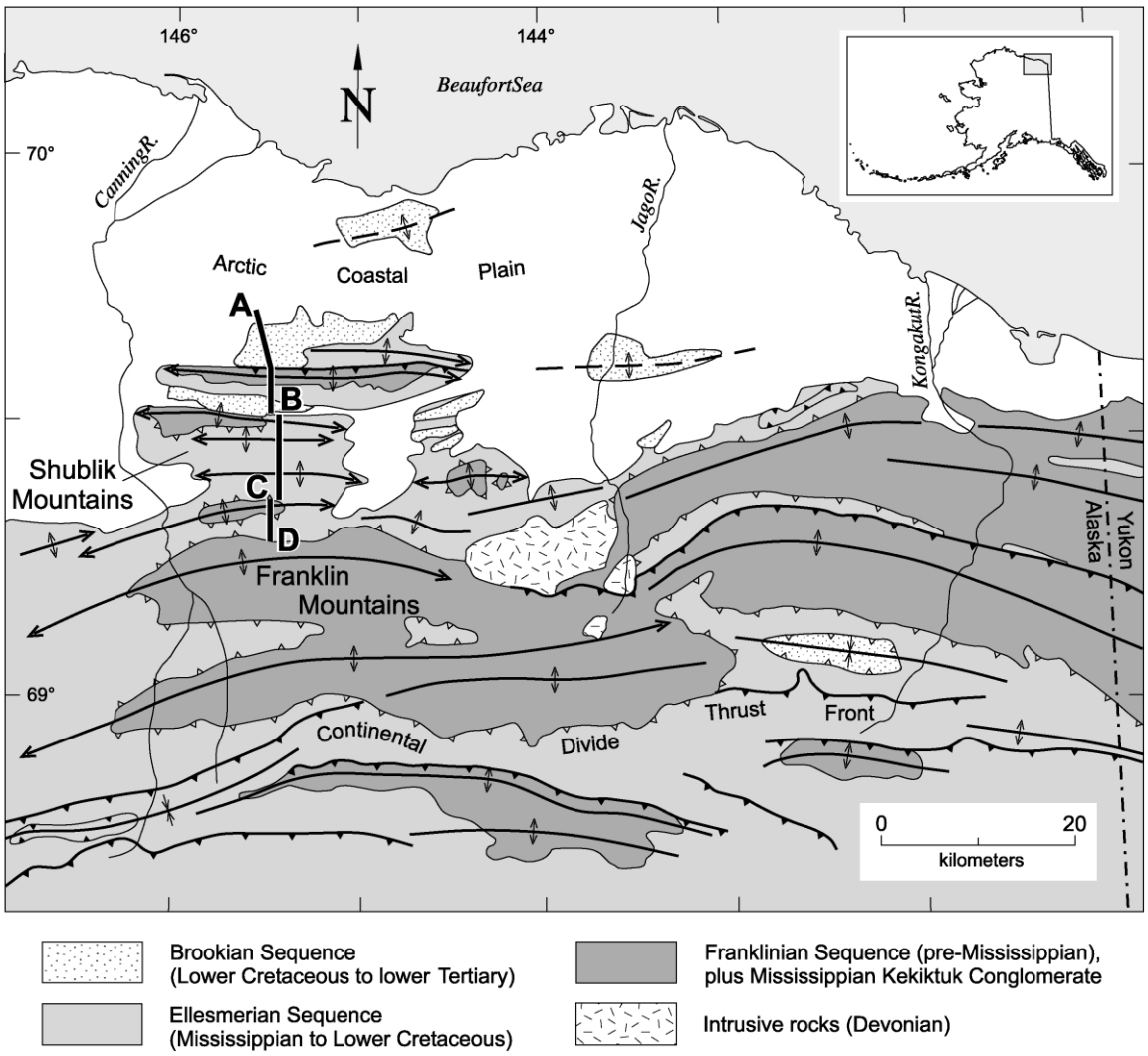

Fig. 1. Generalized tectonic map of northeastern Brooks Range, Alaska, showing line of cross-section in Fig. 3 (ABCD). Modified from Wallace (1993).

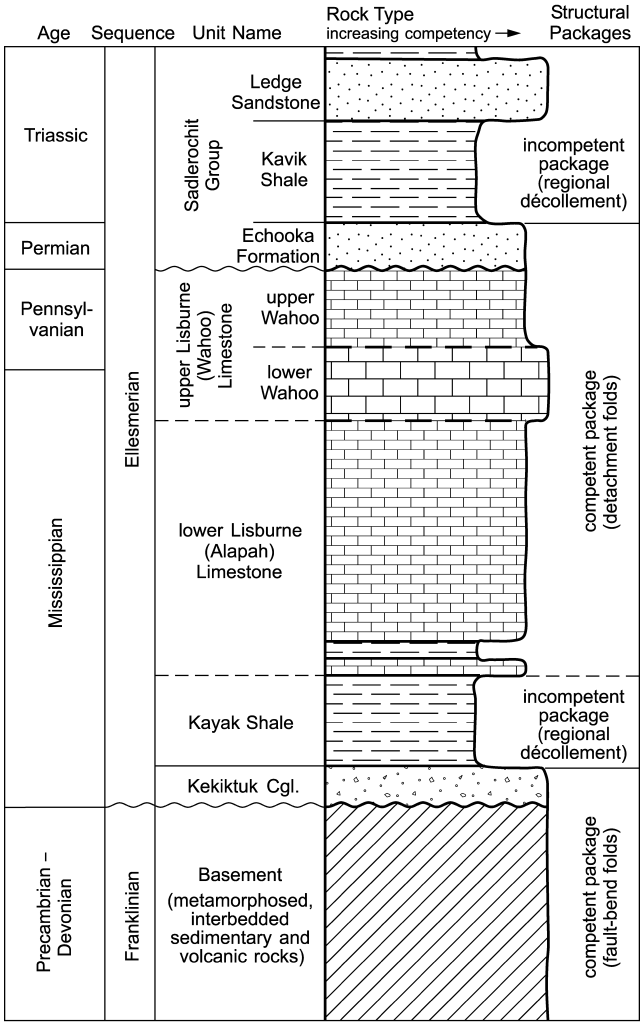

Fig. 2. Schematic stratigraphic column for study areas. Stratigraphy is generalized to emphasize regional mechanical stratigraphy. Relative thicknesses are approximate.

Franklin Mountains of the northeastern Brooks Range are part of the Franklinian and Ellesmerian depositional sequences (Fig. 2) (Bird and Molenaar, 1987). The Franklinian sequence consists of slightly metamorphosed, interlayered sedimentary and volcanic rocks that are Proterozoic to Devonian in age. These rocks are overlain on an angular unconformity by the Ellesmerian sequence, which consists of clastic and carbonate rocks that were deposited on a south-facing passive continental margin. The lower part of this sequence includes the Mississippian Kekiktuk Conglomerate (quartzite), the Mississippian Kayak Shale, and the Carboniferous Lisburne Limestone. The Lisburne Limestone is disconformably overlain by the Permian and Triassic Sadlerochit Group, which includes the Echooka Formation (sandstone), Kavik Shale, Ledge Sandstone, and Fire Creek Siltstone.

In the Shublik and northern Franklin Mountains, the stratigraphic thickness of the Kayak Shale varies between 100 and 200 m, thinning depositionally to the north, and the overlying Lisburne Limestone is ~500 m thick (Gruzlovic, 1991; LePain, 1993; Homza and Wallace, 1997; W.K. Wallace and M.T. Whalen, unpublished measurement, 1999). The lowermost ~300 m of the Lisburne Limestone (formally called the Alapah Limestone) generally consists of 2–10-m-thick packages that grade upward from decimeter-scale beds of mudstone and wackestone to meter-scale beds of packstone and grainstone. The upper ~200 m of the Lisburne (formally called the Wahoo Limestone) can be subdivided into upper and lower parts. The lower ~75 m generally consists of meter-scale beds of packstone and grainstone; this is overlain by ~125 m of meter-scale cycles of grainstone, shale, and muddy dolostone (Gruzlovic, 1991; Whalen, 2000).

2.1.2. Mechanical stratigraphy

On a regional scale, four lithostratigraphic packages define mechanical units relevant to the detachment folds in the northeastern Brooks Range (Fig. 2) (Wallace and Hanks, 1990; Wallace, 1993). These include (a) the Franklinian rocks and the Kekiktuk Conglomerate (together referred to as 'basement' in this paper), which are relatively competent, (b) the Kayak Shale (incompetent), (c) the Lisburne Limestone and Echooka Formation (competent), and (d) the Kavik Shale (incompetent).

Although overall relatively competent compared with the underlying Kayak Shale, the Lisburne Limestone is not a single, mechanically homogeneous unit. On a local scale, the Lisburne Limestone can be subdivided into three thinner mechanical units. The strong and more massive, meter-scale beds of the lower Wahoo are generally separated by poorly-defined slip surfaces and form a relatively competent mechanical unit, while the alternating strong and weak, decimeter-scale beds of the Alapah and upper Wahoo form less competent mechanical units. These three mechanical units are clearly defined by sharp boundaries in some areas, but in other areas the boundaries are gradational and indistinct.

2.1.3. Tectonic and structural setting

The northeastern Brooks Range is a northward salient of the eastern part of the Brooks Range fold-and-thrust belt in Alaska. Unlike the main axis of the Brooks Range, which formed mostly between Middle Jurassic and Paleocene time (Moore et al., 1994; O'Sullivan et al., 1997), shortening and uplift occurred in the northeastern part of the Brooks Range only during the Cenozoic (Wallace and Hanks, 1990; Hanks et al., 1994). This ongoing, north-vergent deformation has led to northward migration of the fold-and-thrust belt, creating large (3–8 km wavelength) fault-bend folds in the basement rocks (Fig. 3) (Wallace and Hanks, 1990; Wallace, 1993). These fault-bend folds form a series of east-trending anticlinoria with gently dipping backlimbs and shorter, more steeply dipping forelimbs. Riding over these waves of fault-bend folds, the Lisburne Limestone has rumpled like a rug, forming shorter-wavelength (0.5–1 km), east-trending detachment

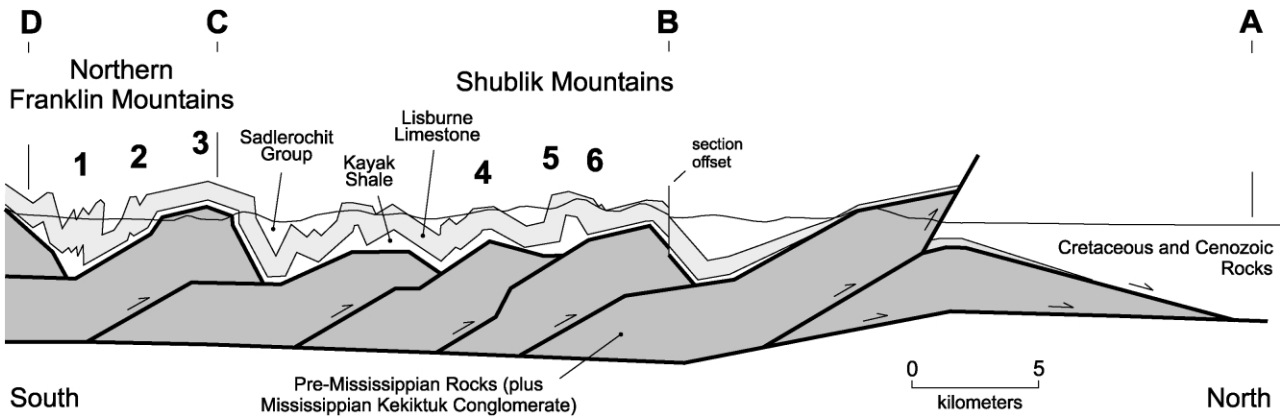

Fig. 3. Generalized cross-section along section line in Fig. 1 showing basement anticlinoria with overlying detachment folds. Numbers mark locations of detachment folds measured in this study. Modified from Wallace (1993).

folds above a regional décollement in the incompetent Kayak Shale. Most of the Sadlerochit Group and overlying units have been eroded away in the Shublik and northern Franklin Mountains, leaving large exposures of folded Lisburne Limestone, with local exposures of basement, Kayak Shale, and the lowermost Sadlerochit Group (Echooka Formation).

2.2. Documentation of fold geometry

We documented and characterized the map-scale geometry of folds in the Lisburne Limestone using a combination of conventional methods, including mapping, photography, and (where possible) direct measurement of attitudes and bed thickness. In order to document map-scale fold shapes and sizes quantitatively, we also surveyed marker horizons in outcrop using a pair of Leica Vector IV reflectorless laser-rangefinder binoculars. The survey data, projected onto a plane perpendicular to the fold axis, allowed construction of profiles with substantially better precision than could be obtained using photographs and map data alone and eliminated distortion resulting from perspective and topographic effects. Nonetheless, significant uncertainties remain because of instrument limitations and gaps in exposures. The horizons surveyed in each fold were largely arbitrary because marker beds are not everywhere well defined, the best marker beds differ between folds, and the entire thickness of Lisburne Limestone is not exposed in any of the folds.

2.3. Fold characteristics and styles of deformation

2.3.1. Observations and results

We documented the geometry of six folds along a north–south transect across the Shublik and northern Franklin Mountains (Fig. 3). Profiles of the folds are shown in Fig. 4 and their geometric characteristics are summarized in Table 1. Folds range from nearly isoclinal with narrow hinge zones (e.g. Fold 1; Fig. 5) to open with wide, rounded hinge zones (e.g. Fold 3; Fig. 6). Other folds have box-fold geometries, in which the zone of curvature change between limbs is a gently dipping panel bounded by two hinges (e.g. Fold 4, southwest ridge; Fig. 7). Folds 1 and 3 are upright, but all others have inclined axial surfaces. Folds 1 and 2 are nearly similar folds, but the others more closely resemble parallel folds. Most of the folds are roughly symmetric; only Fold 2 shows strong asymmetry.

The structural thickness of the Lisburne Limestone varies substantially across individual folds—in the case of Fold 1 (Fig. 5), up to 500%. Structural thickening is evident in both anticlinal and synclinal hinge zones, whereas thickening or thinning may occur in the limbs. These differences in thickness are accommodated in a variety of ways, including combinations of higher-order disharmonic folds, small-scale faults, internal strain, and fracturing. Different parts of the Lisburne locally respond differently to shortening. For example, the Alapah and upper Wahoo are more likely to form higher-order disharmonic folds in fold cores than the lower Wahoo (e.g. anticline in Fold 3 (Fig. 6) and syncline in Fold 5 (Fig. 8)). However, this is not the case everywhere. For example, disharmonic folding is not evident in the core of Fold 1 (Fig. 5) or in the two tight anticlines just south of Fold 1 (which expose the lower Alapah section), nor is disharmonic folding apparent in the synclines immediately north of Folds 1 and 2 (Fig. 4a and b). Small-scale faults exist locally in both the Alapah and Wahoo, and may be either contractional or extensional. The core of Fold 5 is locally thickened by a rabbit-ear (out-of-syncline) thrust fault in the Alapah just below the Wahoo, whereas a small normal fault cuts both the Alapah and Wahoo in the hinge zone of the syncline just north of Fold 2 (Fig. 4b).

The study folds all trend generally eastward with very little plunge, but they are not cylindrical: fold shapes and sizes vary significantly along strike. For example, exposures on opposite sides of a canyon in the south Shublik Mountains show the same folds, less than 1 km apart along strike, with appreciably different shapes (Folds 4 and 5; Fig. 4d and e). Folds 5 and 6 essentially form a single box anticline with a wide crest in the western part of the study area (Fig. 4d), but they are

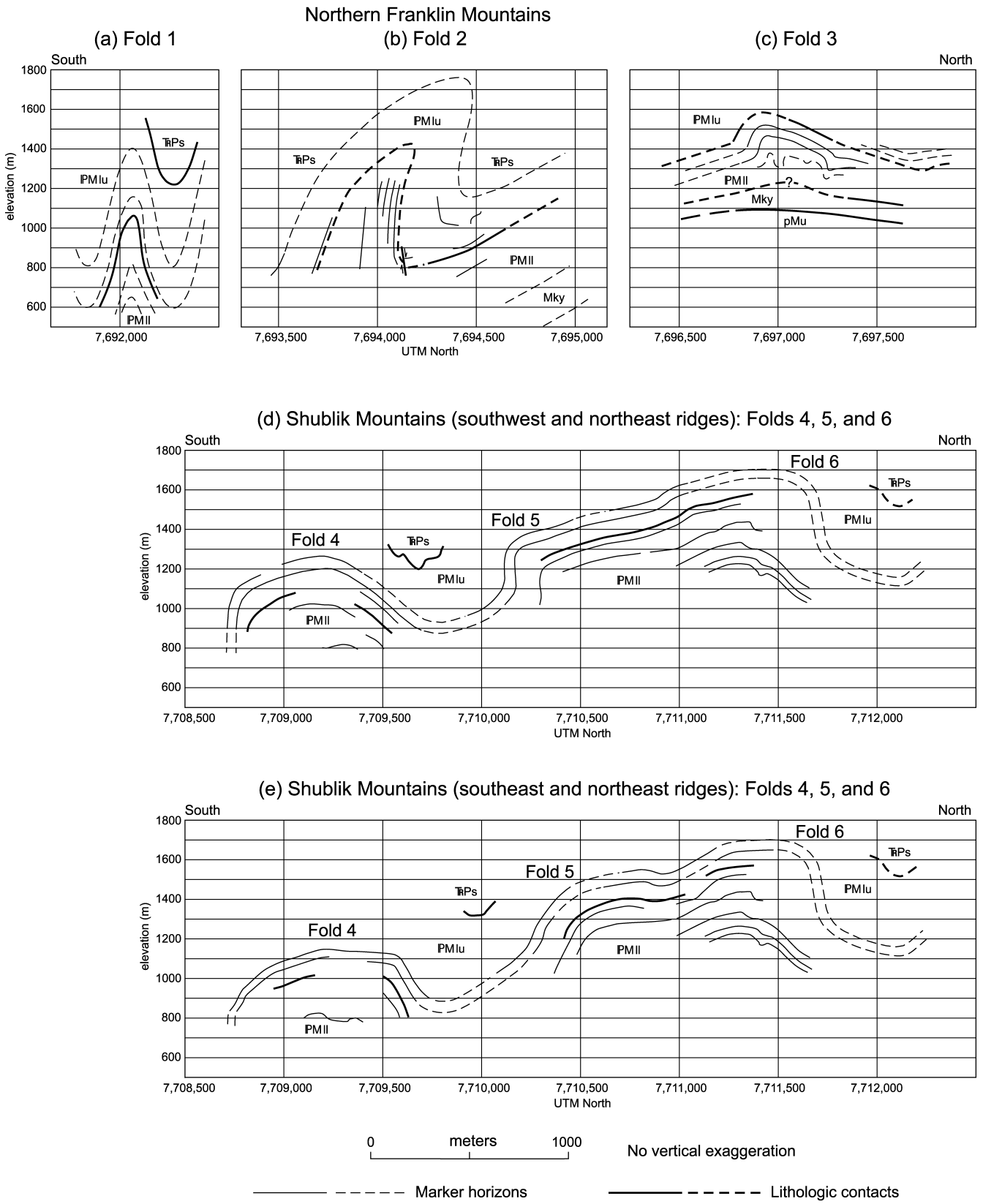

Fig. 4. Profiles of six detachment folds in the northern Franklin Mountains ((a)–(c)) and Shublik Mountains ((d) and (e)). Solid lines are from surveyed points; dashed lines are from field sketches, photographs, and direct measurements. Locations of folds are shown in Fig. 3. TrPs = Echooka Formation of Sadlerochit Group; IPMIu = upper Lisburne Limestone; IPMIl = lower Lisburne Limestone; Mky = Kayak Shale; pMu = pre-Mississippian basement.

Table 1
Measurements of studied folds. Values are rounded to nearest 50 m or 5° to reflect uncertainties in constructing fold profiles

Fold no.	Location		Height (m)	Width (m)	Arc length[a] (m)	Interlimb angle (°)		Height/width	Notes
1	Upper Straight Creek		550	450	1250		15	1.2	Similar; upright; nearly isoclinal
2	Middle Straight Creek		600	400	>1400[b]		35	1.5	Asymmetric; inclined, folded axial surface
3	Lower Straight Creek		150	450	550		90	0.3	Open, rounded
4	South Shublik Mountains	West	600	1150	1800	115–120 (55)[c]		0.5	Parallel; inclined; box fold
		East	450	1100	1550	125–155–160–125 (25)[c]		0.4	Parallel; inclined; rounded, flat-crested
5	South Shublik Mountains	West	300	900	1100		105	0.3	Parallel; inclined; angular
		East	500	850	1100		125	0.6	Inclined; rounded
6	North Shublik Mountains	West	550	750	1250		100	0.7	Parallel; inclined; angular
		East	550	800	1250		100	0.7	Parallel; inclined; angular
5–6	Shublik Mountains (composite)	West	600	1700	2450	105–100 (70)[c]		0.4	Broad box fold
		East	600	1650	2400	125–100 (45)[c]		0.4	Broad box fold, becoming two folds?

[a] Arc length: the length of an individual horizon within the boundaries of a fold.
[b] Forelimb length = 600 m; length of backlimb unknown, but greater than or equal to 800 m.
[c] Multiple hinges within box fold, south to north. Interlimb angle between bounding limbs in parentheses.

Fig. 5. Photograph of Fold 1 (northern Franklin Mountains). This structure is a tight fold with significant thickening in both the anticlinal and synclinal hinge zones, and with thinning in limbs by penetrative internal strain. Lines on photo trace bedding. Fold shape appears different from profile in Fig. 4a due to perspective and topography. Unit symbols as in Fig. 4.

clearly separated into two distinct anticlines by a sharp syncline less than 3 km farther east (Fig. 9).

Because the focus of this study is on map-scale fold geometry, it does not include any quantitative strain analysis. However, our field and thin section observations provide some general insights into the nature and magnitude of strain in the folds. Penetrative strain in both the Alapah and Wahoo has commonly resulted in thinning of the limbs and thickening in the hinge zones of both anticlines and synclines (e.g. Fold 1; Fig. 5). Internal strain is evident in bed thinning or thickening, strained crinoid columns, and mechanical twinning of calcite. Wackestones in the highly thinned limbs of the upper Wahoo of Fold 1 display abundant calcite twins and contain numerous crinoid columns that have been deformed into elliptical cylinders, some of which show elongation of up to 200% in the plane of bedding. Domino-style offsets of crinoid segments also indicate significant shear strain parallel to bedding. Crinoid columns in the thinned southern limb of the upper Wahoo of Fold 5 show similar, but slightly lesser amounts of elongation in the plane of bedding, and twinning is less

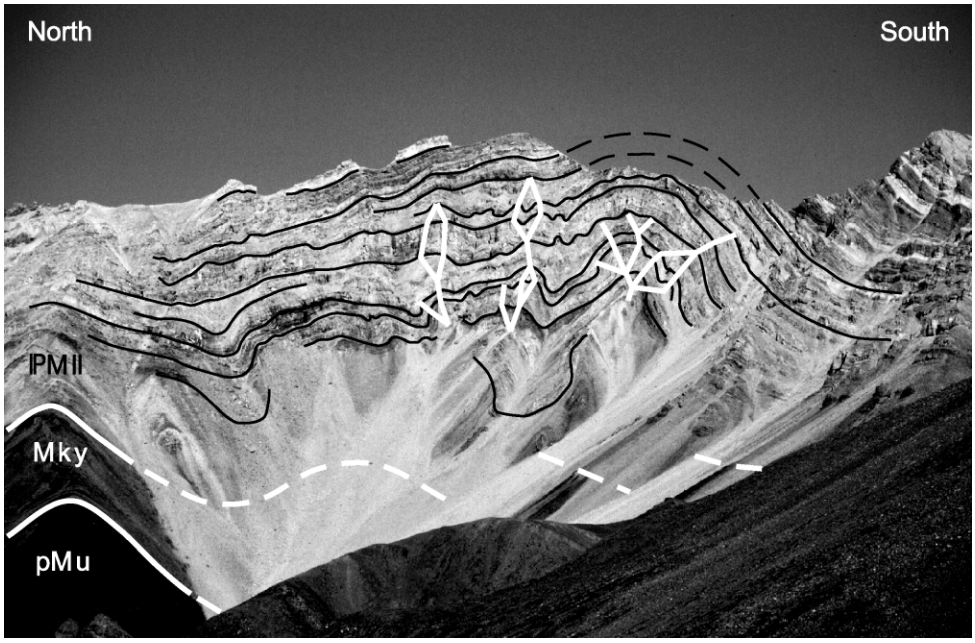

Fig. 6. Photograph of core of Fold 3 (northern Franklin Mountains) showing thickening of lower Lisburne Limestone by higher-order disharmonic folding and internal strain. Black lines trace bedding, while white lines within Lisburne Limestone trace selected hinges, emphasizing their branching and disharmonic nature. Fold shape appears different from profile in Fig. 4c due to perspective and topography. Unit symbols as in Fig. 4.

abundant. Evidence of other mechanisms of deformation in the Lisburne Limestone, including solution cleavage and fracturing, is widespread throughout the study area, but we did not document it in detail.

2.3.2. Discussion

The most important of our observations is that significant changes in competent unit thickness exist across detachment folds in the northeastern Brooks Range over a wide range in shortening. Both anticlinal and synclinal hinge zones display thickening of the competent unit, and limbs may either thin or thicken. These thickness changes are accommodated in a variety of ways, including parasitic folding, internal strain, small-scale faulting, and fracturing. We cannot determine what controls these different responses from our observations alone, but we can suggest some possibilities.

The variable characteristics of the folds and the available evidence about the character and conditions of deformation suggest that fold geometry and evolution were controlled by multiple, interacting factors: (a) the mechanical stratigraphy of the Lisburne Limestone and bounding strata; (b) the relative thicknesses of the Lisburne Limestone and Kayak Shale; (c) the magnitude of total shortening; (d) the

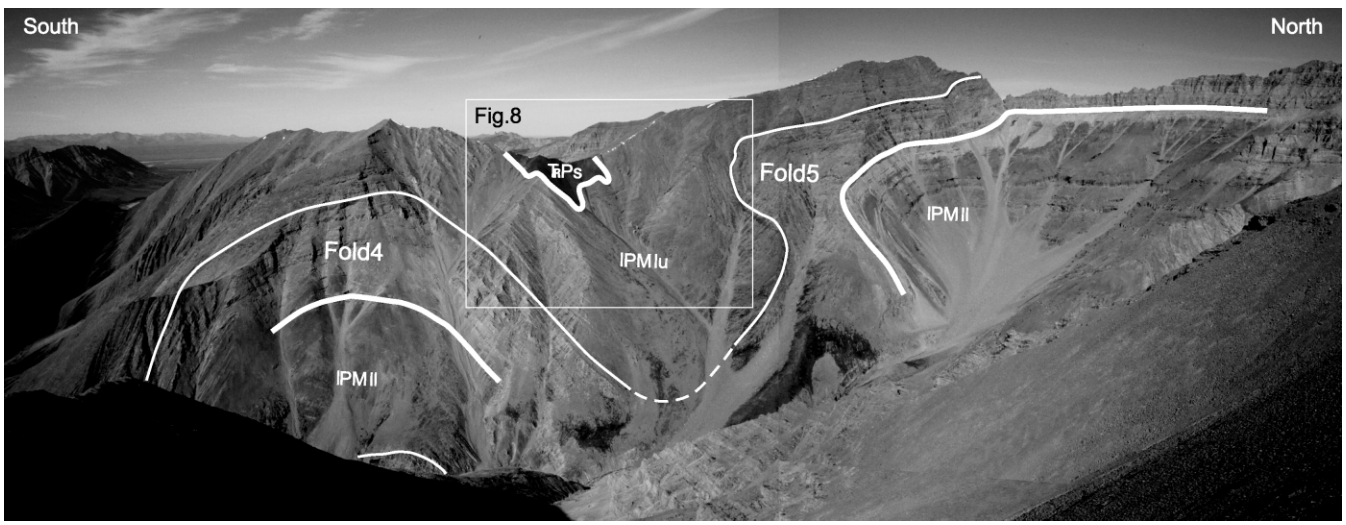

Fig. 7. Photograph of Folds 4 and 5 (Shublik Mountains, southwest ridge). Narrow white line traces marker horizon in upper Lisburne Limestone. Fold shapes appear different from profile in Fig. 4d due to perspective and topography. Unit symbols as in Fig. 4.

Fig. 8. Photograph of syncline between Folds 4 and 5 (Shublik Mountains, southwest ridge), showing thickening in upper Lisburne Limestone by parasitic folding. Unit symbols as in Fig. 4.

geometry and evolution of the basement structure; and (e) the conditions of deformation, especially temperature.

The mechanical stratigraphy within the Lisburne Limestone played a significant role in the character of folding. The less competent Alapah and upper Wahoo mechanical units, which are composed of relatively thin (decimeter-scale) beds separated by weak slip surfaces, formed higher-order folds along these minor décollements, or they formed approximately parallel first-order folds by flexural slip. Conversely, the massive, thicker, and stronger beds of the lower Wahoo show no higher-order folding and tend to have deformed primarily by flexural slip and/or internal strain, as indicated by widely-spaced, bed-parallel slip surfaces and thickness changes.

Differences in competency and stratigraphic thickness between the Lisburne Limestone and the underlying Kayak Shale likely affected the style of folding as well, and may help explain why the Alapah and upper Wahoo form

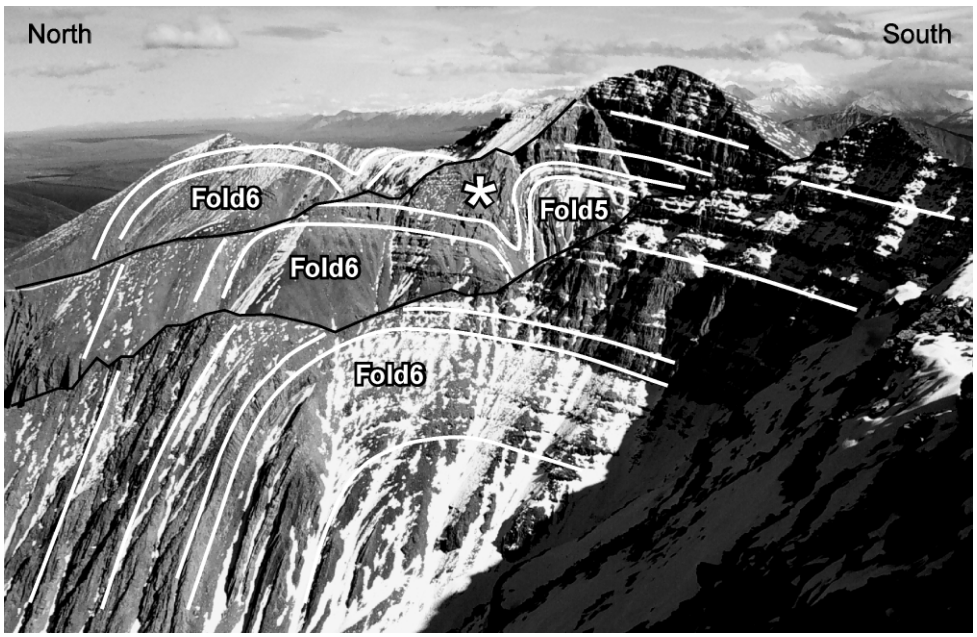

Fig. 9. Photograph of eastward continuation of Folds 5 and 6 (north Shublik Mountains). View is along strike to east, across three ridges (outlined in black). Syncline marked by asterisk clearly divides Fold 6 from Fold 5. Farther west, Folds 5 and 6 are essentially one large box fold.

higher-order folds in some places, but not in others. The Kayak Shale is relatively incompetent, and thus is able to migrate into the cores of developing anticlines from the adjacent synclinal hinge zones (Homza and Wallace, 1997). This could allow the fold to grow in the Lisburne by flexural slip while maintaining parallel folding with constant bed length and thickness. However, this could continue throughout the growth of the fold only where the Kayak Shale is sufficiently thick in the synclinal hinge zones to accommodate the initial increase in area of the core of the growing anticline and thus maintain constant area (assuming no movement of material into or out of the plane of cross-section). The Kayak Shale is generally much thinner than the Lisburne, but its stratigraphic thickness is apparently quite variable (20–40% of the Lisburne thickness). In those areas where it is thinnest (e.g. Fold 3 and Folds 4–6) and insufficient incompetent material was available to fill the core of the growing anticline, the Lisburne would be forced to thicken, resulting in disharmonic folding in the Alapah. Disharmonic folds are either uncommon or entirely absent in the cores of folds where the Kayak is thicker and thus was able to fill the growing anticline core (e.g. Folds 1 and 2).

Our best estimates of fold height-to-width ratios range from 0.3 to 1.5; fold heights range from 150 to 600 m, widths range from 400 to 1700 m, and interlimb angles range from 15 to 125° (Table 1). The magnitude of total shortening cannot be estimated without considerable uncertainty because of data limitations, but we can compare relative shortening using interlimb angles to quantify bending of the competent unit. According to this measure, the dominant mechanism of folding in the competent Lisburne Limestone generally changes with increased shortening. Flexural slip usually dominates in the initial stages of shortening at larger interlimb angles, but shortening is increasingly accommodated by penetrative internal strain (e.g. Fold 1) and/or small-scale faulting as interlimb angles decrease. That is, flexural slip may be progressively superseded by fold flattening as interlimb angles decrease and folds lock due to some combination of increasing interlayer angular shear and decreasing fold cross-sectional area (e.g. Ramsay, 1967; Bhattacharya, 1992; Homza and Wallace, 1997). The initial flexural slip can occur either in parallel first-order folds or disharmonic parasitic folds. For example, Fold 1 shows no evidence of parasitic folding, whereas in Fold 3, substantial initial thickening of the Lisburne Limestone is accommodated by parasitic folds that probably formed largely by flexural slip.

Fold shapes and the distribution of structural thickening/thinning in the Lisburne Limestone may be partially explained by the structural topography on the top surface of the basement anticlinoria (Fig. 3). In particular, the inclined axial surfaces of many of the folds are a direct consequence of their position over the inclined limbs of these anticlinoria. Folds tend to be more open over the crests and limbs of anticlinoria, whereas folds tend to be tighter and reflect greater shortening in the cores of the synclinoria between basement horses. In addition, as basement horses were emplaced beneath the cover, the weak coupling between basement and cover may have favored the formation of symmetrical detachment folds in the cover (Davis and Engelder, 1985). The initial displacement of the basement horses likely created relief above the horses, and shortening of the cover between horses could have structurally thickened the incompetent Kayak Shale in the synclinoria. These two factors probably initiated and promoted the early, rapid growth of detachment folds in the Lisburne in the synclinoria, and the thickened Kayak allowed these folds to form with few or no parasitic folds (e.g. Fold 1). The folds that developed later over the crests and inclined limbs of the rising basement horses likely developed on a thinner layer of Kayak Shale and were more likely to accommodate layer-parallel shortening by parasitic folding in the Alapah in the anticline core (e.g. Fold 3).

The environmental conditions during burial also had an important influence on the mode of folding. Total stratigraphic overburden in the study area was at most slightly over 5 km, and possibly much less (Bird and Molenaar, 1987). However, thermal alteration at ~190–350 °C indicated by conodont analyses from the Lisburne Limestone in the study area (A.P. Krumhardt, written communication, 2000) suggests substantially deeper burial depths of 7–14 km, which would require significant structural thickening. Higher temperatures would favor increasingly ductile behavior of even the more competent beds in the carbonates of the Lisburne, thus reducing competency contrasts and allowing a greater variety of deformation mechanisms to operate (e.g. mechanical twinning, dissolution creep, dislocation creep, and grain boundary creep). The clear and widespread evidence of shortening by penetrative strain indicates that at least the later stages of fold evolution occurred at elevated temperatures.

Although we cannot directly document the kinematic evolution of the six folds we studied, their geometries provide a few clues—and raise new questions—about their evolution. Most notably, arc lengths do not systematically increase with decreasing interlimb angles (Table 1). This suggests that the competent Lisburne Limestone was not fed into the fold in order to maintain constant area as the fold tightened, and consequently that the bounding synclinal hinges did not migrate. In addition, several folds display box-fold geometries, with wide hinge zones defined by relatively flat panels. However, the evolution of the hinges bounding these panels is unknown, so it is unclear how the width of the panels may have varied during fold growth. The west and east ridge profiles of Folds 4–6 (Fig. 4d and e) show that hinges can develop or disappear over short distances along strike; in some cases, they can develop into major fold hinges that divide a single anticline into two (e.g. Folds 5 and 6; Figs. 4d and e and 9). Hinge evolution, including how hinge zones vary in width as a fold develops,

significantly affects area balance and hence has important consequences in modeling the evolution of folds.

3. Modeling the geometry and evolution of detachment folds

3.1. Existing conceptual models

Geologists have long debated how detachment folds form, and have proposed a number of conceptual models to explain the geometric and kinematic evolution of these folds (e.g. Wiltschko and Chapple, 1977; Dahlstrom, 1990; Epard and Groshong, 1995; Poblet and McClay, 1996; Homza and Wallace, 1997). Table 2 compares major characteristics and assumptions for the four major categories of models. All assume area balance, but they differ on other major points. Perhaps the most long-lived and controversial issue has been whether fold hinges are fixed or whether they migrate with respect to the rock (see Poblet and McClay (1996) for discussion). Some recent studies, including Fischer et al. (1992), Anastasio et al. (1997), and Homza and Wallace (1997), provide evidence for fixed hinges; others, such as Stewart and Alvarez (1991), Zapata and Allmendinger (1996), and Suppe et al. (1997), find evidence that some hinges migrate. Both probably occur in nature under different conditions and with varying controlling factors.

We interpret the folds we studied to have grown with no competent Lisburne Limestone feeding through the outer boundaries of the fold as it tightened. This would mean that at least the synclinal hinges did not migrate significantly, and is consistent with the findings of Homza and Wallace (1997). We therefore focused our analysis only on the two models in which migrating hinges are not required to maintain area balance—namely, the models described by Homza and Wallace (1995, 1997), and by Groshong and Epard (1994) and Epard and Groshong (1995). These two models differ substantially in their assumptions regarding changes in bed length and bed thickness during fold evolution. The Homza and Wallace (1997) model (Fig. 10a) assumes a distinct contrast in layer competency, reflected by the competent unit maintaining constant length and thickness throughout the folding process. However, this requires the incompetent unit initially to thin and then to thicken in the synclines in order to balance the changing area of incompetent material in the anticline core.

At the other end of the spectrum, the Epard and Groshong (1995) model (Fig. 10b) effectively treats the entire section as a mechanically homogeneous unit by assuming a geometrically uniform response throughout the fold. It assumes that constant area is maintained during fold evolution strictly through layer-parallel shortening or extension in all units. Thickness in the synclines does not change, so constant detachment depth is maintained.

Table 2
Comparison of models for the geometry and kinematics of detachment folds, showing major characteristics and assumptions used for each

Model	Major characteristics and assumptions					
	Hinges	Limb length	Limb dip	Depth to detachment	Bed length	Mechanical layering
Poblet and McClay (1996) 'Model 1'	Migrating, non-rotating	Variable	Constant	Constant	Constant	Constant-thickness competent layer overlies incompetent layer
Dahlstrom (1990)	Migrating, rotating	Variable	Variable	Constant	Constant	Constant-thickness competent layer overlies incompetent layer
Homza and Wallace (1995, 1997)	Non-migrating, rotating	Constant	Variable	Variable	Constant	Constant-thickness competent layer overlies incompetent layer
Epard and Groshong (1995)	Non-migrating, rotating or migrating, rotating	Variable	Variable	Constant	Variable	Homogeneous, with variable thickness
Hybrid Model (this paper)	Non-migrating, rotating or migrating, rotating	Variable	Variable	Variable	Variable	Variable-thickness competent layer overlies incompetent layer

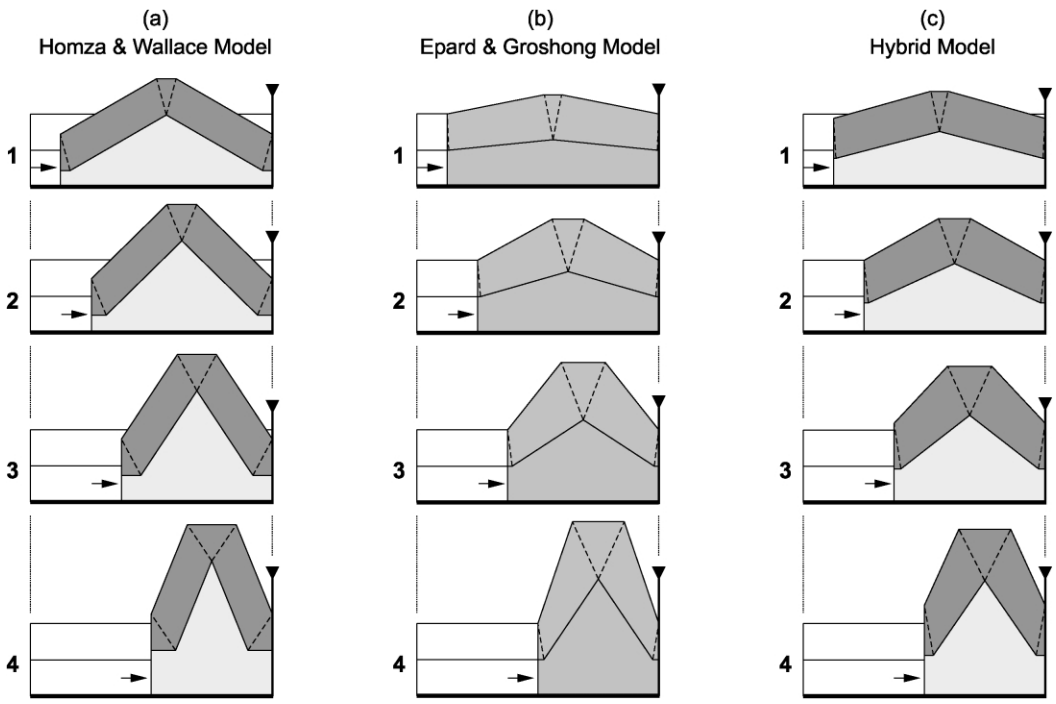

Fig. 10. Comparison of three models describing the geometry and kinematics of detachment folds. Competent units are dark gray; incompetent units are light gray (Epard and Groshong model does not differentiate between competent and incompetent units). Horizontal, parallel lines show initial unit thicknesses. (a) Homza and Wallace model. Fold maintains constant area and constant competent unit length and thickness. Incompetent unit initially thins greatly under synclinal hinges, then thickens as material is expelled from anticline core, producing a variable depth to detachment. (b) Epard and Groshong model. Fold maintains constant area strictly through layer-parallel shortening in all units, which thicken only in the anticline (between the synclinal hinge zones). (c) Hybrid model. Fold maintains constant area by a combination of varying depth to detachment (as in (a)), and thickness change in the competent unit in both the anticline (as in (b)) and the syncline.

3.2. A new conceptual model

The variations in structural competency, structural thickness, and detachment depth observed in detachment folds in the northeastern Brooks Range indicate that some of the assumptions employed by both the Homza and Wallace and Epard and Groshong models are inappropriate for the observed folds. We therefore propose a new model that specifically accommodates variations in mechanical stratigraphy, competent unit thickness, and detachment depth (Table 2; Fig. 10c). This model incorporates elements from both the Homza and Wallace and Epard and Groshong models, and in many respects is simply a hybrid between the two (i.e. the Homza and Wallace and Epard and Groshong models are specific end-member cases of this more general model). It is important to emphasize at the outset that this model can provide a description of fold geometry that more completely and realistically matches natural detachment folds, but it cannot prescribe the kinematic evolution that led to a particular fold geometry unless assumptions are made to constrain that evolution.

As in both of the existing models, the 'hybrid model' assumes constant cross-sectional area, but unlike the Homza and Wallace model, it does not assume constant bed length and thickness in the competent unit (Fig. 10). The essential contrast with the Epard and Groshong model is that thickness change is not uniform throughout the stratigraphic column, but is assumed to be less in the 'competent' unit than in the 'incompetent' unit in order to reconstruct the geometric consequences of differences in competency. In the Epard and Groshong model, shortening uniquely determines limb dip for any given stratigraphic level, whereas in the hybrid model limb dip depends on the relative amounts of shortening accommodated by thickness change in the competent and incompetent units. As in the Homza and Wallace model, constant area of the incompetent unit is maintained in the hybrid model by redistribution of material between synclinal hinge zones and anticline cores, resulting in changes in incompetent unit thickness. In natural folds, the relative change in thickness of the competent and incompetent units depends on various factors, including competency contrast between the competent and incompetent units, and increasing resistance to interlayer slip in tightening folds. In contrast with both existing models, the hybrid model allows thickness to change in the syncline in both the incompetent and competent units.

Given specified hinge locations, the Epard and Groshong and Homza and Wallace models each uniquely predict the evolution of a fold. In contrast, the hybrid model does not restrict the evolution of a fold to a single fixed kinematic path, but, by allowing different amounts of bed shortening and thickness changes, can represent the full spectrum from a single mechanically homogeneous unit (as in the Epard

and Groshong model) to units of extreme competency contrast, with the overlying competent unit maintaining constant bed length and thickness (as in the Homza and Wallace model).

Appendix A discusses the mathematical relationships between the three models, and Appendix B outlines the mathematics needed to construct a basic hybrid model with flat panels and thickening in the hinge zones.

Figs. 11–15 show examples of the Homza and Wallace, Epard and Groshong, and hybrid models with box-fold and sinusoidal geometries. In order to maintain constant bed thickness in the competent unit, the Homza and Wallace model requires hinge zones that consist of flat panels bounded by hinges that rotate as shortening increases. However, such hinge zones are not a requirement of either the Epard and Groshong or the hybrid models. Neither of these models constrain the location, orientation, or evolution of hinges in anticlines, nor does the hybrid model constrain the hinges in synclines.

3.3. Evaluations and comparisons of the models

In order to explore the effects of different assumptions on these three models, we developed a set of computer programs that simulate the geometric and kinematic development of a symmetrical fold for each model. Evaluations using these programs clearly highlight differences between the models, as well as limitations of the models. Different parameters, such as the relative initial thicknesses of the competent and incompetent units, and initial arc lengths relative to stratigraphic thicknesses, can result in very different (and sometimes impossible) geometries using even the same model. Figs. 11–13 illustrate some of these differences for generic, symmetrical folds. All of these illustrations assume that the variables affecting fold kinematics, such as the rate of thickening of the competent unit, remain constant throughout fold evolution. This is only a simplifying assumption for the purposes of modeling, and is not required or even likely to

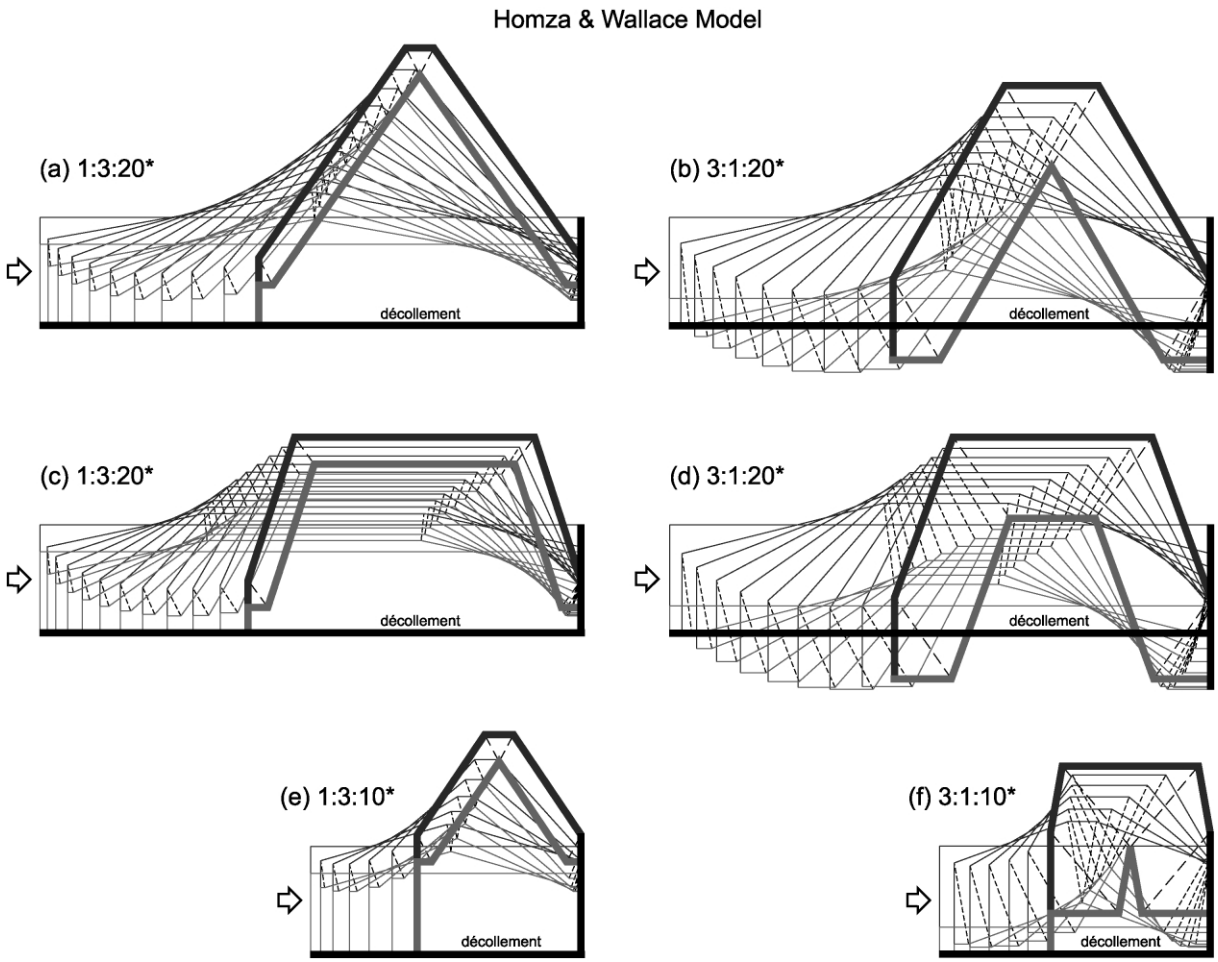

Fig. 11. Geometric and kinematic characteristics of detachment folds using the Homza and Wallace model. A relatively long arc length with thicker competent unit than incompetent unit ((b) and (d)) causes the fold to bottom out because incompetent material in synclinal hinge zones is insufficient to fill the rapidly expanding anticline core. Geometries with a wide, flat panel at the fold crest ((c) and (d)) require more thinning of the incompetent unit in synclinal hinge zones to accommodate a larger area in the core. A relatively short arc length with a thicker competent unit than incompetent unit (f) results in a box fold after relatively little shortening, in contrast with a fold in which the competent unit is thinner than the incompetent unit (e). For comparison purposes, all folds in Figs. 11–13 are drawn to the same scale and show 40% final shortening. *Ratio of initial values of upper unit thickness:lower unit thickness:arc length.

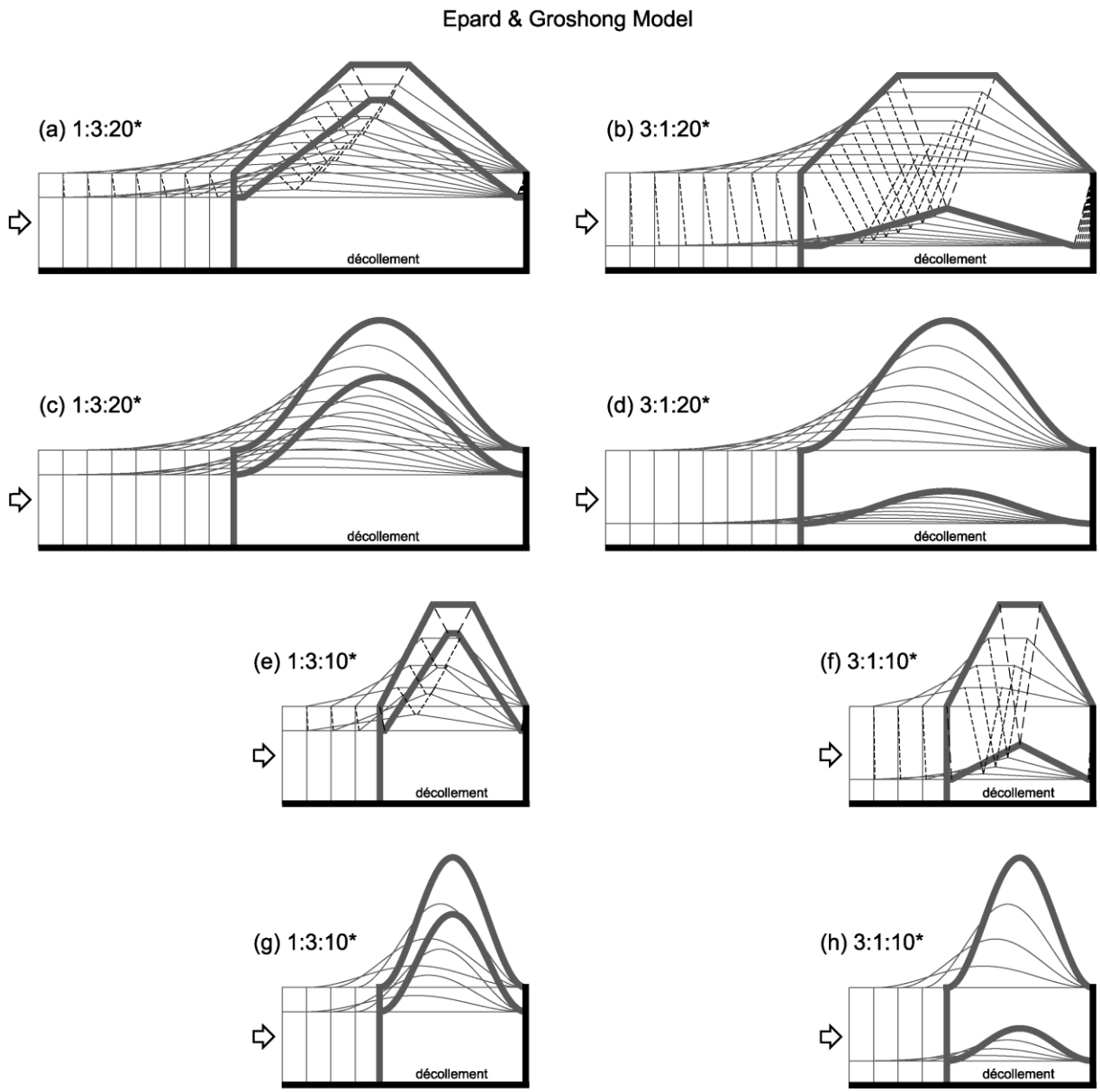

Fig. 12. Geometric and kinematic characteristics of detachment folds using the Epard and Groshong model. Sine curves and flat panels in anticlinal hinge zones are a departure from the Epard and Groshong model *sensu stricto*, but yield more realistic geometries at greater shortening. Cores of anticlines thicken significantly, with large differences in amplitude between the upper and lower horizons, especially for folds with relatively high initial unit thickness to arc length ratios ((f) and (h)). For comparison purposes, all folds in Figs. 11–13 are drawn to the same scale and show 40% final shortening. *Ratio of initial values of upper unit thickness:lower unit thickness:arc length.

apply to natural folds. Neither the Epard and Groshong nor the hybrid models constrain the hinges that bound flat panels in the hinge zone, so the kinematic models include arbitrary assumptions about how these panels change in width as the fold evolves. Appendix B contains examples of the mathematical formulae we used.

Fig. 11a, c and e shows that the Homza and Wallace model works reasonably well as long as the competent unit is sufficiently thin relative to the underlying incompetent unit. However, if the competent unit is sufficiently thick and/or long, then the fold 'bottoms out', requiring it to lock or change its mode of evolution. In Fig. 11b and d, for example, horizontal displacement cannot proceed according to the model past the first stage shown since no more incompetent material is available to fill the expanding core. Anticlines with a flat panel in the hinge zone at the boundary between competent and incompetent units exacerbate this problem because they result in a larger area in the core that must be filled with incompetent material (Fig. 11c and d). The Homza and Wallace model also cannot easily accommodate folds with high ratios of competent unit thickness to arc length, as these folds become isoclinal with relatively little horizontal

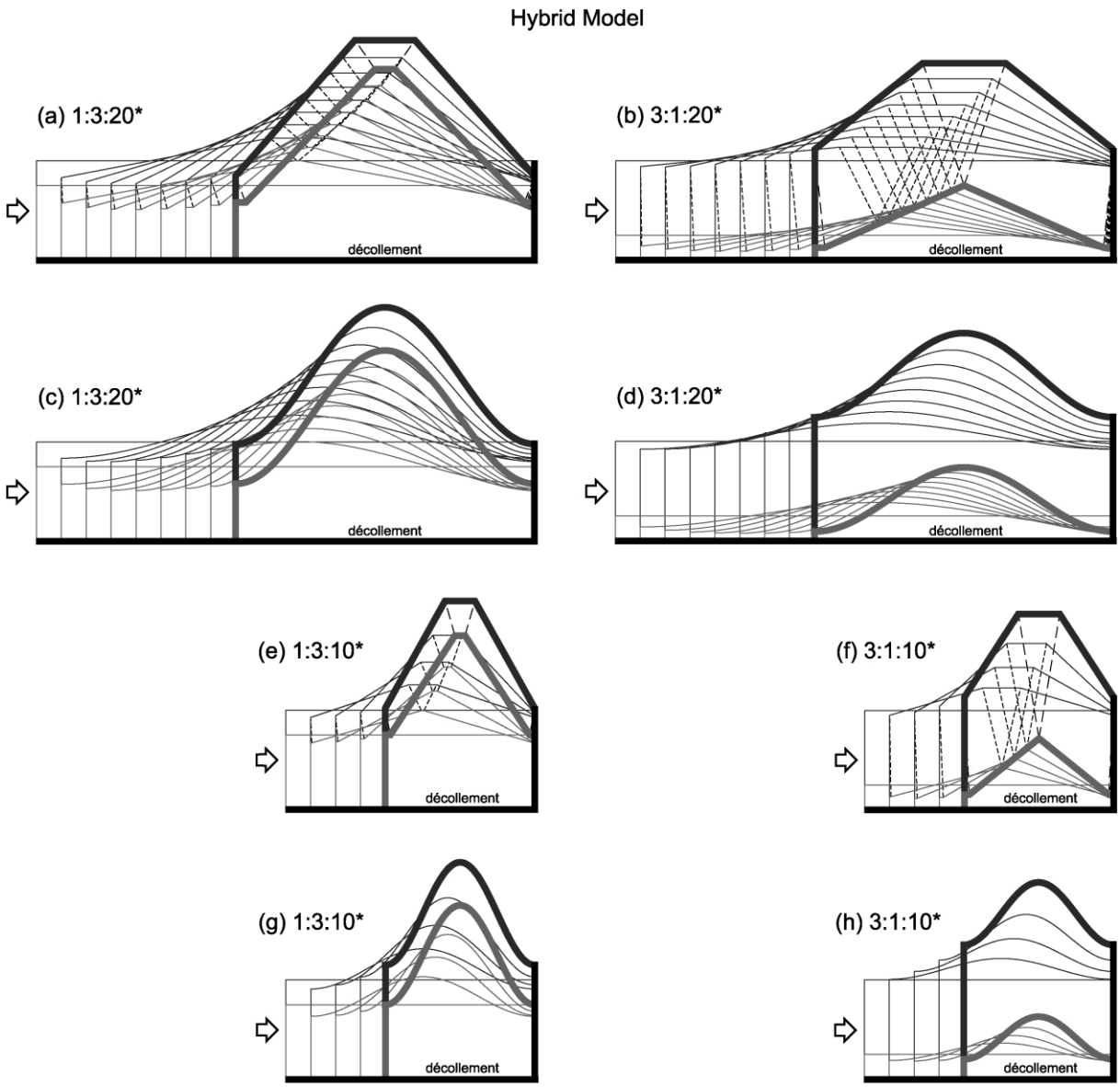

Fig. 13. Geometric and kinematic characteristics of detachment folds using hybrid model with sine curves and flat panels in anticlinal hinge zones. Thickening of the upper competent unit moderates extreme thinning of the incompetent unit in synclines required by the Homza and Wallace model. However, the hybrid model allows less thickening in the competent unit than does the Epard and Groshong model, and it allows thickening in hinge zones of both anticlines and synclines, which distributes thickness changes more evenly through the competent unit. For comparison purposes, all folds in Figs. 11–13 are drawn to the same scale and show 40% final shortening. *Ratio of initial values of upper unit thickness:lower unit thickness:arc length.

displacement (Fig. 11f). Displacement and heightening of these folds can proceed further only by thinning the limbs and thickening the hinge zones in the competent unit, which violate the model's assumptions of constant thickness and length of the competent unit.

Both the Epard and Groshong and hybrid models (Figs. 12 and 13) avoid these problems because they relax the requirement of constant competent unit thickness and length. At comparable low magnitudes of horizontal displacement, both of these models result in folds with lower amplitude than the Homza and Wallace model. However, high magnitudes of displacement can result in extremely amplified anticlinal hinge zones with unrealistically sharp geometries unless a flat panel is introduced in the hinge zone. With the Epard and Groshong model, this is particularly true for folds with high thickness to arc length ratios. Even with box-fold or sinusoidal geometries, such folds display extreme thickening toward the hinge zone, with large differences in amplitude between the upper and lower horizons (e.g. Fig. 12f and h). The hybrid model allows moderation of these extremes by decreasing the amount of competent unit thickening in the anticlinal hinge zones and/or increasing it in the synclinal hinge zones (Fig. 13f and h).

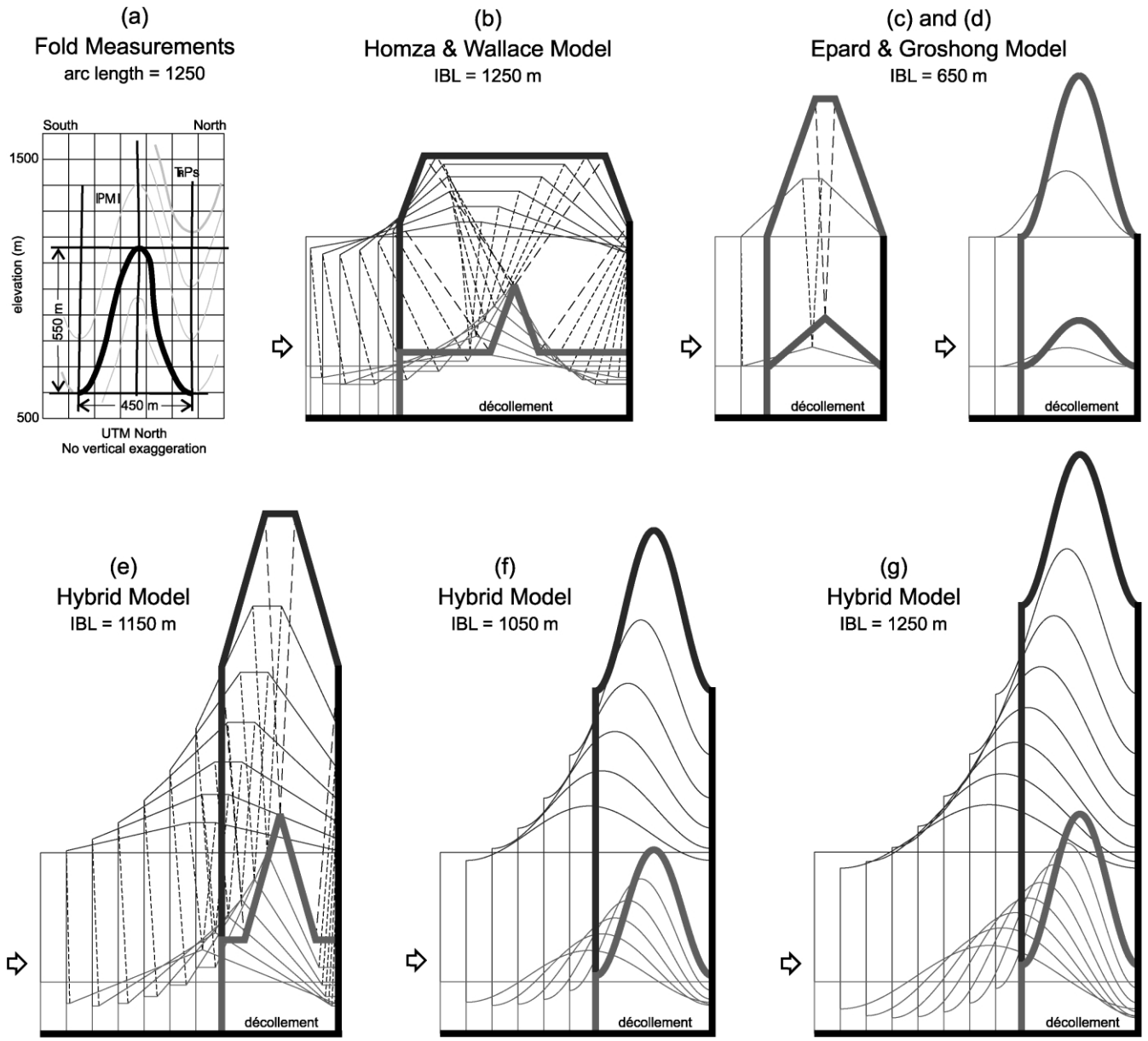

Fig. 14. Geometric and kinematic analysis of Fold 1 (northern Franklin Mountains) using the Homza and Wallace, Epard and Groshong, and hybrid models. All folds are drawn to the same scale. Surveyed measurements (a) show final geometry of a horizon in upper Lisburne Limestone. Initial stratigraphic thicknesses used for the competent and incompetent units are 500 and 200 m, respectively; initial bed lengths (IBL) are noted for each of the models. The Homza and Wallace model (b) cannot duplicate the large height:width ratio of the fold because it requires the fold to grow wider rather than taller; the fold becomes isoclinal and locks well before it reaches the required final width of 450 m. Epard and Groshong model ((c) and (d)) predicts significantly different line lengths of upper and lower horizons and extreme thickening in anticlinal hinge zone but no thickening in synclinal hinge zones; both are inconsistent with observed geometry. Final geometries produced by the hybrid model ((e)–(g)) better match those of the actual fold, particularly if curves are used. The amount of structural thickening of the competent Lisburne Limestone is not entirely known, so a range of initial bed lengths is possible; however, the initial bed length required by the hybrid model is always less than or equal to that required by the Homza and Wallace model, and greater than that required by the Epard and Groshong model. In (e), thickening initially is entirely in the synclinal hinge zone to illustrate the flexibility of the hybrid model in how thickness changes are distributed throughout the fold.

3.4. Application of conceptual models to natural folds

We developed the hybrid model to take into account certain characteristics we observed in natural folds, particularly thickness changes in the competent unit. The model was not created to reproduce the geometry of the observed folds in detail, but rather as a conceptual tool to explore the consequences of relaxing some of the assumptions incorporated in previously published models for detachment folds. The next obvious question is whether the model does, in fact, describe the characteristics of natural detachment folds better than those models. The characteristics we documented from representative examples of our study folds provide an opportunity to test

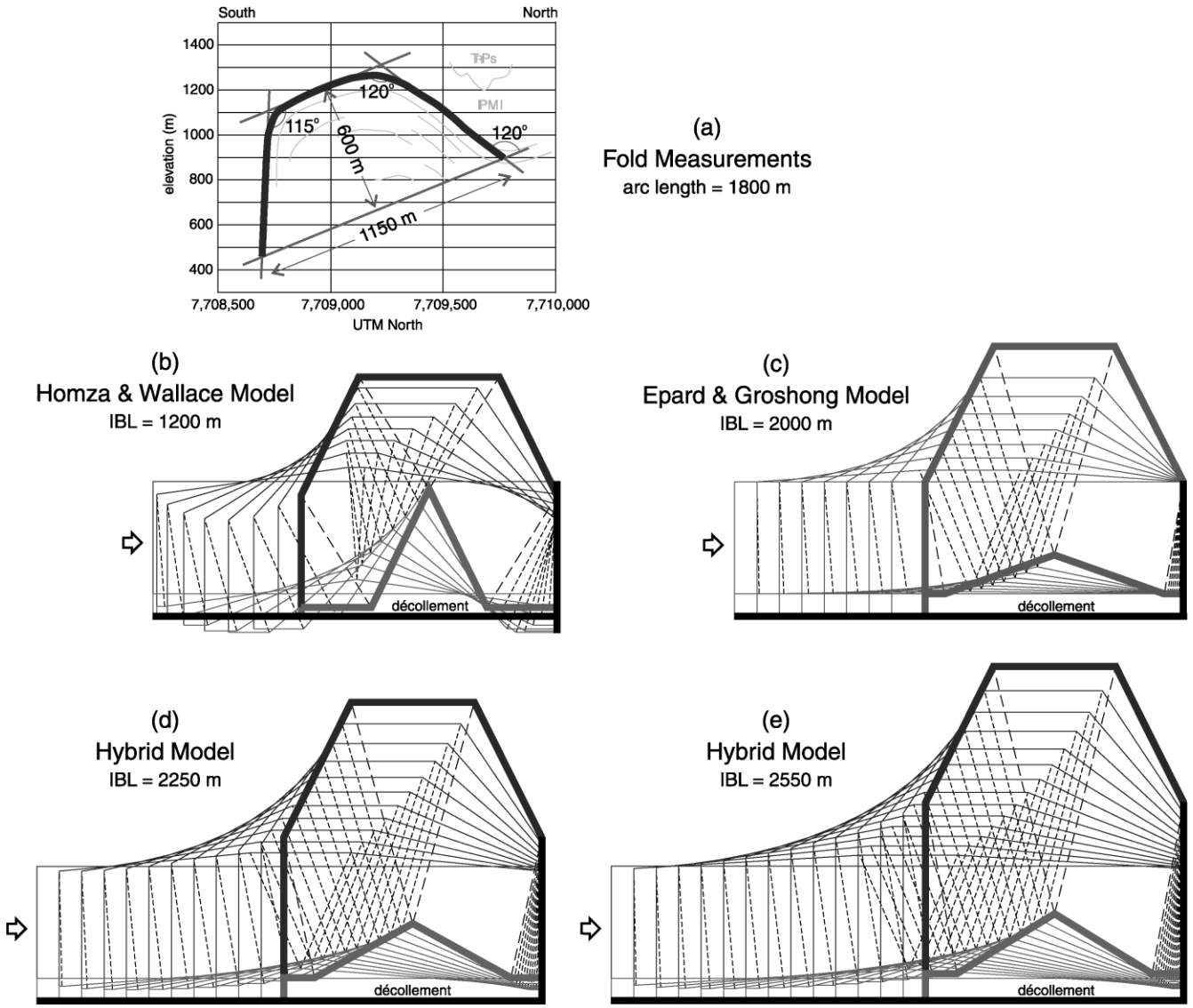

Fig. 15. Geometric and kinematic analysis of Fold 4 (Shublik Mountains, southwest ridge) using the Homza and Wallace, Epard and Groshong, and hybrid models. All folds are drawn to the same scale. Surveyed measurements (a) show final geometry of a horizon in upper Lisburne Limestone. The fold has been tilted over the south-dipping backlimb of a basement horse. Initial stratigraphic thicknesses used for the competent and incompetent units are 500 and 100 m, respectively; initial bed lengths (IBL) are noted for each of the models. The Homza and Wallace model (b) cannot duplicate the final height of the fold, and it bottoms out after $<3\%$ shortening due to insufficient incompetent material. With flat panels at the crest, the Epard and Groshong and hybrid models can duplicate the fold's final geometry ((c)–(e)), but the Epard and Groshong model (c) does not duplicate observed thickening of the competent unit in the synclinal hinge zone. Thickening in both the anticlinal and synclinal hinge zones in the hybrid model ((d) and (e)) requires longer initial bed lengths than do either the Homza and Wallace or Epard and Groshong models. The final structural thickness of the Lisburne Limestone is unknown, so the initial bed lengths are indeterminate; (d) and (e) illustrate two possibilities.

the Homza and Wallace, Epard and Groshong, and hybrid models against natural folds. Even the best of our profiles do not provide sufficient information for unambiguous fold reconstruction because of incomplete exposure and analytical uncertainty in our survey data. Nevertheless, the survey-based profiles provide reconstructions of fold geometry that are quantitatively better constrained than profiles derived from map information alone, which typically serve as the basis for analysis of map-scale fold geometry.

Fig. 14 compares models for Fold 1, and Fig. 15 compares models for Fold 4. The Homza and Wallace model produces obviously unrealistic geometries for both of these folds. In fact, it simply cannot duplicate Fold 1, with its large ratios of height to width and competent to incompetent unit thicknesses, because the fold is forced to grow wider rather than taller in order to maintain the assumed constant bed thickness (Fig. 14b). Moreover, according to the Homza and Wallace model, the fold becomes isoclinal and thus locks well before it can shorten to the observed 450 m width of Fold 1. Nor does the Homza and Wallace model work for Fold 4 with its high initial ratio of arc length to incompetent unit thickness, since the model

requires much more thinning of the Kayak Shale than is possible. According to the model, the competent unit bottoms out and locks against the décollement with less than 3% displacement (Fig. 15b).

The Epard and Groshong model (Figs. 14c and d and 15c) can produce final shapes similar to those observed near the top of the competent unit in both of the natural folds. However, the natural folds do not meet several of the fundamental assumptions of this model. For example, the Lisburne Limestone and the Kayak Shale are not equally competent and thus do not respond as a single mechanically homogeneous unit. Also, in most (if not all) of the folds we studied, the Lisburne Limestone has thickened considerably in both the anticlinal and synclinal hinge zones. Although this study did not document structural thickness changes in the Kayak Shale, Homza and Wallace (1997) showed that detachment folds in the northeastern Brooks Range also violate the assumption that detachment depth remains constant.

The hybrid model can reconstruct final geometries that match these natural folds quite well, that do not bottom out prematurely, and that include differences in thickening that are consistent with mechanical contrasts between layers. The hybrid model allows reconstructions of Fold 1 with nearly similar geometries that display thinning in the limbs and thickening in both anticlinal and synclinal hinge zones (Fig. 14e–g). These do not involve significant layer-parallel shortening in the early phases of folding, which is consistent with the absence of parasitic folding in Fold 1. By contrast, the Epard and Groshong model cannot reproduce similar geometries and involves significant layer-parallel shortening from the beginning of folding. Reconstructions of Fold 4 with the hybrid model (Fig. 15d and e) require layer-parallel shortening of the competent unit throughout the fold because of its longer arc length and to avoid bottoming out due to the thinner Kayak Shale in the Shublik Mountains. These display layer-parallel shortening of the competent unit similar to the Epard and Groshong end member, but differ in their substantial thickening in the synclinal hinge zones.

3.5. Implications and limitations of the hybrid model

The hybrid model allows competent unit thickness and length to vary in both anticlinal and synclinal hinge zones, allows detachment depth to vary, and does not constrain the geometry and evolution of the hinge zone. This flexibility allows the hybrid model to provide a better match than other models to the final geometry of the natural folds we used as examples, but it also introduces distinct limitations. In particular, the model allows an infinite array of possibilities for the geometry and evolution of a fold and thus cannot be used to uniquely reconstruct either the geometry of unseen parts of a fold or the kinematic evolution of a fold. To narrow the range of geometric or kinematic possibilities requires additional information, such as that derived from mechanical modeling and/or observations that constrain the geometry and kinematic steps in the evolution of natural folds. Despite this limitation of the model as a predictive tool, it can still provide a more realistic reconstruction of natural folds than models that include inappropriate simplifying assumptions, and can serve as a tool to explore the sensitivity of fold geometry and kinematics to different variables.

Our comparisons of the application of different models to natural examples of folds illustrate the importance of model assumptions in estimates of total shortening. The hybrid model may improve estimates of total shortening if appropriate measurements of competent unit thickening can be obtained. Correct thicknesses in the anticlinal and synclinal hinge zones are especially critical in determining total shortening. However, hinge zones are not commonly exposed in their entirety, so the available information allows a range in estimated shortening. For example, in Fold 4 (Fig. 15d and e), initial arc lengths of 2250 and 2550 m, combined with slightly different effective competency contrast, allow virtually identical final geometries at the top of the competent unit, with the main difference in final fold geometry being in the thicknesses of anticlinal and synclinal hinge zones. In Fold 1 (Fig. 14e–g), similar final geometries, but with different thicknesses in the anticlinal and synclinal hinge zones, are possible using initial arc lengths anywhere between 1050 and 1250 m. The anticlinal and synclinal hinge zones are clearly thickened in both of these natural folds, but it is not possible to determine total shortening uniquely unless we know the amount of thickening.

Despite this limitation of the hybrid model, estimates of total shortening using the Homza and Wallace or Epard and Groshong models may be even more inaccurate if the simplifying assumptions of the models are not applicable. For example, significantly more displacement is required for Fold 4 by the hybrid model than by the Epard and Groshong model (with thickening only in the anticlinal hinge zone) or by the Homza and Wallace model (with no thickening in either anticlinal or synclinal hinge zones). For Fold 1, the hybrid model still requires more shortening than the Epard and Groshong model, but it requires either the same or slightly *less* shortening than the Homza and Wallace model. Thus, shortening calculations based on either of the existing models may result in substantial under- or overestimates, depending on the particular characteristics of individual folds. This obviously has important implications for the effect of simplifying assumptions on the accuracy of tectonic reconstructions. If appropriate measurements can be obtained, the hybrid model may help improve shortening estimates for individual folds. However, it is much more difficult to envision how to address practically the effects of variable thickness on shortening estimates at the scale of a tectonic reconstruction that includes many folds.

Comparison of the different models with natural folds emphasizes the importance of accurately determining

thickness changes. Conventional techniques of tracing contacts and locating data points using a topographic map alone generally lack sufficient resolution to quantify thickness changes across map-scale folds. Techniques that facilitate accurate reconstruction of fold shape, such as dip isogons (Ramsay and Huber, 1987), are also only useful if enough data points are both physically accessible and precisely located. Surveying techniques and, where physical access allows, GPS surveys and conventional thickness measurements provide practical methods to quantify changes in thickness across folds at map scale. Even where practical considerations preclude use of such approaches, our comparison of models suggests some ways to obtain more accurate reconstructions of map-scale fold geometry, and hence better estimates of shortening. These include estimating unit thickness in the hinge zone, locating the hinges that bound the hinge zone as precisely as possible, and determining the difference in limb dip between the upper and lower contacts of a unit.

Finally, it is important to emphasize that, like the Homza and Wallace and Epard and Groshong models, the hybrid model is a two-dimensional model that attempts to explain a three-dimensional structure. The fact that the folds in the northeastern Brooks Range vary in character along strike emphasizes that their geometry and evolution are very complex. The development of a fold must certainly depend on what happens in all directions, not just in a vertical plane in the direction of maximum displacement. Nevertheless, understanding how folds evolve in two dimensions is an essential step toward understanding the more complex problem of folding in three dimensions.

4. Conclusions

We have analyzed the geometry of six map-scale detachment folds in the northeastern Brooks Range in detail. The most important observation to emerge from this analysis is that significant changes in competent unit thickness can exist across detachment folds over a wide range in shortening. Thickening of the competent unit is common in both anticlinal and synclinal hinge zones, and limbs may either thin or thicken. Thickness changes may be accommodated in various ways, including parasitic folding, internal strain, small-scale faulting, and fracturing. Some of these thickness changes are visually obvious, but others are not. Methods such as surveying better document these changes quantitatively; conventional mapping alone generally lacks sufficient resolution.

The character, distribution, and amount of thickness change may be controlled by multiple interacting factors, including the mechanical stratigraphy of the competent Lisburne Limestone and its bounding strata, the relative thicknesses of the competent Lisburne Limestone and the incompetent Kayak Shale, the geometry and evolution of the underlying basement surface, the burial history, and the total shortening.

Our results are consistent with earlier observations by Homza and Wallace (1997) that detachment folds in the northeastern Brooks Range evolved with fixed hinges (i.e. material did not feed through hinges into or out of the folds) and with variable detachment depth (i.e. change in structural thickness of the incompetent unit).

Previously published end-member conceptual models for the geometry and kinematic evolution of fixed-hinge detachment folds do not adequately explain all of the observed characteristics of the northeastern Brooks Range folds. The model of Homza and Wallace (1995, 1997) assumes constant bed length and thickness in the competent unit. Folds formed according to this model will bottom out if the incompetent unit is not sufficiently thick, and space problems increase with increasing competent-unit thickness. The Epard and Groshong model (Groshong and Epard, 1994; Epard and Groshong, 1995) assumes uniform competency throughout the fold, no thickness change in the competent unit in the synclinal hinge zone, and constant detachment depth. This model predicts a progressive increase in limb dip upward in anticlines that is inconsistent with some observed folds, especially at high magnitudes of shortening.

We propose a hybrid model that relaxes some of the assumptions of the end-member models to fit the observed characteristics of natural folds. This hybrid model allows competent unit thickness and length to vary in both anticlinal and synclinal hinge zones, allows detachment depth to vary, and does not constrain the geometry and evolution of the hinge zone. This flexibility allows the hybrid model to provide a better match to the final geometry of natural folds, but it also precludes a unique reconstruction of either the geometry of unseen parts of a fold or the kinematic evolution of a fold. Nonetheless, the model provides a convenient tool to explore how changes in specific variables may affect the geometry and kinematics of a fold.

The simplifying assumptions incorporated in the Homza and Wallace and Epard and Groshong models, such as constant competent unit thickness and constant detachment depth, are violated by natural detachment folds in the northeastern Brooks Range, and probably by comparable folds elsewhere in the world. Use of these assumptions for these folds can lead to significant error in shortening estimates. The hybrid model, while still a simplification, can yield better estimates of shortening by allowing structural changes in competent unit thickness in both anticlinal and synclinal hinge zones and variation in detachment depth.

Our results emphasize the importance of accurately determining thickness changes across map-scale folds. This may require conventional geological mapping to be supplemented with quantitative methods such as surveying and conventional thickness measurements. Where such approaches are not practical, the results of conventional

mapping may be improved by estimating unit thickness in the hinge zone, locating hinges that bound the hinge zone as precisely as possible, and determining the difference in limb dip between the upper and lower contacts of a unit.

Acknowledgements

D.J. Anastasio, M.S. Wilkerson, and an anonymous reviewer provided helpful comments on the manuscript. This project was funded by the U.S. Department of Energy, contract DE-AC26-98BC15102.

Appendix A. Relationships between models

Here we present the mathematical relationships between arc length, bed thickness, horizontal displacement, and limb dip in the Epard and Groshong (1995), Homza and Wallace (1997) and hybrid models. These relationships are for a symmetrical detachment fold with flat-bottomed synclines and a triangular anticline at the contact between the upper and lower units, as shown in Fig. A1. The relationships apply to the lower unit and its contact with the upper unit:

$$b = \frac{l_0 - d}{2} - g \tag{A1}$$

$$a = \left(\frac{l_0 - d}{2} - g\right)\tan\theta \tag{A2}$$

$$a = \sqrt{\left(\frac{l_f}{2} - g\right)^2 - \left(\frac{l_0 - d}{2} - g\right)^2} \tag{A3}$$

where l_0 = initial arc length (initial bed length between synclinal hinges), l_f = final arc length at upper–lower unit boundary, d = amount of horizontal displacement (shortening), g = length of synclinal flat panel at base of upper unit, θ = limb dip at upper–lower unit boundary, and a, b, and c are as shown in Fig. A1. Assuming conservation of area, where the area before folding equals the area after folding, then:

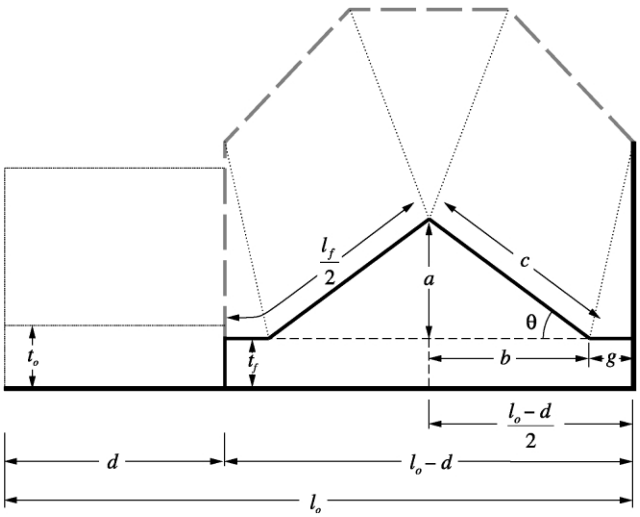

Fig. A1. Area-balanced diagram of generic symmetrical detachment fold with triangular anticline and flat-bottomed synclines at contact between upper and lower units.

$$l_0 t_0 = ab + t_f(l_0 - d) \tag{A4}$$

where t_0 = initial lower unit thickness, and t_f = final lower unit thickness at synclinal hinges. Substituting Eqs. (A1) and (A2) into Eq. (A4) and solving for θ yields:

$$\theta = \arctan\left[\frac{l_0 t_0 - t_f(l_0 - d)}{\left(\frac{l_0 - d}{2} - g\right)^2}\right] \tag{A5}$$

Substituting Eqs. (A1) and (A3) into Eq. (A4) and solving for t_f yields:

$$t_f = \frac{l_0 t_0 - \left(\frac{l_0 - d}{2} - g\right)\sqrt{\left(\frac{l_f}{2} - g\right)^2 - \left(\frac{l_0 - d}{2} - g\right)^2}}{l_0 - d} \tag{A6}$$

If initial unit thickness (t_0) and arc length (l_0) are known, the Epard and Groshong and Homza and Wallace models each uniquely predict the evolution of a fold. Since $t_f = t_0$ in the Epard and Groshong model, a change in d in Eq. (A5) yields a unique dip for the upper–lower unit boundary. Likewise, in the Homza and Wallace model $l_f = l_0$ so a change in d in Eq. (A6) results in a unique final thickness of the incompetent unit at the synclinal hinges while conserving area. In the hybrid model, neither l_f nor t_f necessarily must equal l_0 or t_0, respectively, so Eqs. (A5) and (A6) do not yield unique solutions. As a result, the hybrid model does not restrict the evolution of a fold to a single fixed kinematic path.

Appendix B. Building the hybrid model

The mathematical relationships presented in Appendix A can be augmented to build a hybrid model that includes an upper unit with either a triangular or flat-crested geometry. Operations are added successively to define the length of the boundary between the upper and lower units, the length of the synclinal flat panel, the amount of thickening in the synclinal hinge zones, and the length of the anticlinal flat panel. These quantities are determined by formulae and scaling factors chosen by the user based on observations and/or assumptions about fold geometry and evolution. The scaling formulae we have provided here are merely examples of what can be used.

B.1. Lower unit geometry (Fig. A1)

To adjust the length of the horizon between the upper and lower units, let l_f vary as $l_0 - [x(l_0 - l_{epard})]$ where x is a user-defined scaling factor, and $(l_0 - l_{epard})$ is the difference between the Homza and Wallace ($l_0 = l_f$) and Epard and Groshong (l_{epard}) final arc lengths. The difference in final arc lengths determined here can be used to approximate the competency contrast between the upper and lower units; i.e. length closer to that of Homza and Wallace (l_0) = higher contrast; length closer to that of Epard and Groshong (l_{epard}) = lower contrast.

To adjust the length of the synclinal flat panel, let g vary as yd where y is a user-defined scaling factor.

B.2. Upper unit triangular geometry (Fig. A2)

Before folding:

$$\text{Area}_{\text{total}} = \text{Area}_{\text{lower unit}} + \text{Area}_{\text{upper unit}} = l_0 t_0 + l_0 u \quad \text{(A7)}$$

After folding:

$$\text{Area}_{\text{total}} = 2\text{Area}_{\Delta\text{ABE}} + 2\text{Area}_{\text{rectangle BCDE}} = h\left(\frac{l_0 - d}{2}\right) + 2\left(\frac{l_0 - d}{2}\right)(t_f + u) \quad \text{(A8)}$$

Assuming conservation of area, we can equate Eqs. (A7) and (A8) and solve for h:

$$h = \frac{2l_0}{l_0 - d}(t_0 + u) - 2(t_f + u) \quad \text{(A9)}$$

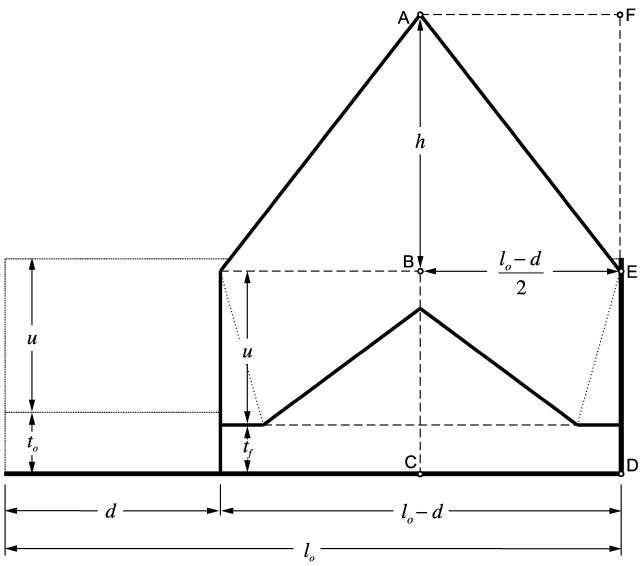

Fig. A2. Area-balanced diagram of generic symmetrical detachment fold with triangular anticlinal crest.

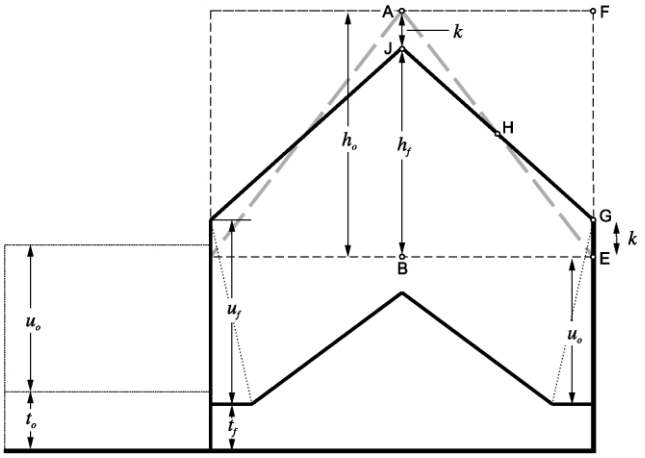

Fig. A3. Area-balanced diagram of generic symmetrical detachment fold showing geometric construction of thickening in synclinal hinge zones.

B.3. Thickening in synclinal hinge zones (Fig. A3)

Since AB||FE and AJ = GE, $\text{Area}_{\Delta\text{AJH}} = \text{Area}_{\Delta\text{EGH}}$ and thus:

$$\text{Area}_{\text{trapezoid JBEG}} = \text{Area}_{\Delta\text{ABE}} \quad \text{(A10)}$$

To adjust the amount of thickening in the synclinal hinge zones, let k vary as $z((h_0 + u_0)/2)$ where z is a user-defined scaling factor. From Fig. A3:

$$h_f = h_0 - k \quad \text{(A11)}$$

$$u_f = u_0 + k \quad \text{(A12)}$$

B.4. Anticlinal flat panel (Fig. A4)

To adjust the length of the anticlinal flat panel, let q_0 vary as $w((dl_0 - d^2)/l_0)$ where w is a user-defined scaling factor. From Fig. A4:

$$r_0 = \left(\frac{l_0 - d}{2}\right) - q_0 \quad \text{(A13)}$$

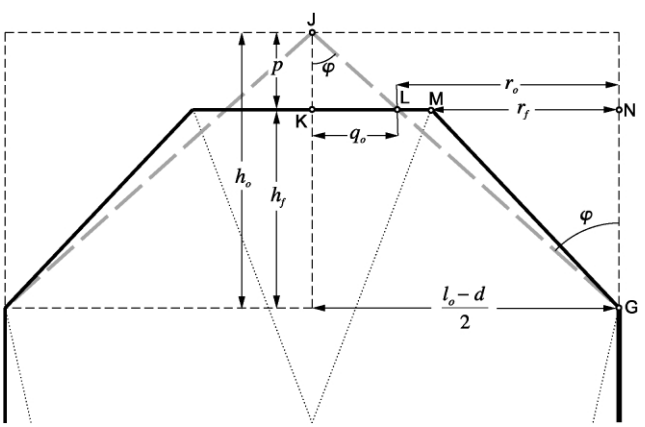

Fig. A4. Detail of upper unit of fold in Fig. A1 showing geometric construction of flat crest in anticline. Diagram is area balanced.

$$h_f = \frac{r_0}{\tan\varphi} \quad \text{(A14)}$$

where φ = half the interlimb angle. Assuming conservation of area:

$$\text{Area}_{\Delta LGM} = \text{Area}_{\Delta JKL} \quad \text{(A15)}$$

From Fig. A4:

$$\text{Area}_{\Delta LGM} = \text{Area}_{\Delta LGN} - \text{Area}_{\Delta MGN} \quad \text{(A16)}$$

Substituting Eq. (A15) into Eq. (A16) and solving for r_f:

$$\text{Area}_{\Delta JKL} = \text{Area}_{\Delta LGN} - \text{Area}_{\Delta MGN} \quad \text{(A17)}$$

$$\frac{pq_0}{2} = \frac{r_0 h_f}{2} - \frac{r_f h_f}{2} \quad \text{(A18)}$$

$$r_f = r_0 - \frac{pq_0}{h_f} \quad \text{(A19)}$$

References

Anastasio, D.J., Fisher, D.M., Messina, T.A., Holl, J.E., 1997. Kinematics of décollement folding in the Lost River Range, Idaho. Journal of Structural Geology 19, 355–368.

Bhattacharya, A.R., 1992. A quantitative study of hinge thickness of natural folds; some implications for fold development. Tectonophysics 212, 371–377.

Bird, K.J., Molenaar, C.M., 1987. Stratigraphy of the northern part of the Arctic National Wildlife Refuge, northeastern Alaska. In: Bird, K.J., Magoon, L.B. (Eds.), Petroleum Geology of the Northern Part of the Arctic National Wildlife Refuge, Northeastern Alaska. U.S. Geological Survey Bulletin 1778, pp. 37–59.

Dahlstrom, C.D.A., 1990. Geometric constraints derived from the law of conservation of volume and applied to evolutionary models for detachment folding. American Association of Petroleum Geologists Bulletin 74, 336–344.

Davis, D.M., Engelder, T., 1985. The role of salt in fold-and-thrust belts. Tectonophysics 119, 67–88.

Epard, J.-L., Groshong, R.H. Jr, 1995. Kinematic model of detachment folding including limb rotation, fixed hinges and layer-parallel strain. Tectonophysics 247, 85–103.

Fischer, M.P., Jackson, P.B., 1999. Stratigraphic controls on deformation patterns in fault-related folds: a detachment fold example from the Sierra Madre Oriental, northeast Mexico. Journal of Structural Geology 21, 613–633.

Fischer, M.P., Woodward, N.B., Mitchell, M.M., 1992. The kinematics of break-thrust folds. Journal of Structural Geology 14, 451–460.

Groshong, R.H., Epard, J.-L., 1994. The role of strain in area-constant detachment folding. Journal of Structural Geology 16, 613–618.

Gruzlovic, P.D., 1991. Stratigraphic evolution and lateral facies changes across a carbonate ramp and their effect on parasequences of the carboniferous Lisburne group, Arctic National Wildlife Refuge, northeastern Alaska. M.S. thesis, University of Alaska Fairbanks.

Hanks, C.L., Wallace, W.K., O'Sullivan, P.B., 1994. The Cenozoic structural evolution of the northeastern Brooks Range, Alaska. In: Thurston, D., Fujita, K. (Eds.), 1992 Proceedings International Conference on Arctic Margins, U.S. Minerals Management Service Outer Continental Shelf Study 94-0040, pp. 263–268.

Homza, T.X., Wallace, W.K., 1995. Geometric and kinematic models for detachment folds with fixed and variable detachment depths. Journal of Structural Geology 17, 575–588.

Homza, T.X., Wallace, W.K., 1997. Detachment folds with fixed hinges and variable detachment depth, northeastern Brooks Range, Alaska. Journal of Structural Geology 19, 337–354.

Jamison, W.R., 1987. Geometric analysis of fold development in overthrust terranes. Journal of Structural Geology 9, 207–219.

LePain, D.L., 1993. Transgressive sedimentation in rift-flank region: deposition of the Endicott Group (Early Carboniferous), northeastern Brooks Range, Alaska. Ph.D. thesis, University of Alaska Fairbanks.

Moore, T.E., Wallace, W.K., Bird, K.J., Karl, S.M., Mull, C.G., Dillon, J.T., 1994. Chapter 3. Geology of northern Alaska. In: Plafker, G., Berg, H.C. (Eds.), The Geology of Alaska: The Geology of North America, v. G1. Geological Society of America, Boulder, Colorado, pp. 49–140.

O'Sullivan, P.B., Murphy, J.M., Blythe, A.E., 1997. Late Mesozoic and Cenozoic thermotectonic evolution of the central Brooks Range and adjacent North Slope foreland basin, Alaska: including fission track results from the Trans-Alaska Crustal Transect (TACT). Journal of Geophysical Research 102 (B9), 20,821–20,845.

Poblet, J., Hardy, S., 1995. Reverse modeling of detachment folds; application to the Pico de Aguilla anticline in the South Central Pyrénées (Spain). Journal of Structural Geology 17, 1707–1724.

Poblet, J., McClay, K., 1996. Geometry and kinematics of single-layer detachment folds. American Association of Petroleum Geologists Bulletin 80, 1085–1109.

Ramsay, J.G., 1967. Folding and Fracturing of Rocks, McGraw Hill, New York, 568pp.

Ramsay, J.G., Huber, M.I., 1987. The Techniques of Modern Structural Geology, Volume 2: Folds and Fractures, Academic Press, New York, 392pp.

Stewart, K.G., Alvarez, W., 1991. Mobile-hinge kinking in layered rocks and models. Journal of Structural Geology 13, 243–259.

Suppe, J., Sabat, F., Muñoz, J., Poblet, J., Roca, E., Verges, J., 1997. Bed-by-bed fold growth by kink-band migration: Sant Llorenç de Morunys, eastern Pyrénées. Journal of Structural Geology 19, 443–461.

Wallace, W.K., 1993. Detachment folds and a passive-roof duplex: examples from the northeastern Brooks Range, Alaska. In: Solie, D.N., Tannian, F. (Eds.), Short notes on Alaskan Geology. Alaska Division of Geological and Geophysical Surveys Professional Report 113, pp. 81–99.

Wallace, W.K., Hanks, C.L., 1990. Structural provinces of the northeastern Brooks Range, Arctic National Wildlife Refuge, Alaska. American Association of Petroleum Geologists Bulletin 74, 1100–1118.

Whalen, M.T., 2000. Baseline stratigraphy of the Lisburne Group. In: The Influence of Fold and Fracture Development on Reservoir Behavior of the Lisburne Group of Northern Alaska, First Annual Report. United States Department of Energy Award DE-AC26-98BC15102, pp. B1–B14.

Wiltschko, D.V., Chapple, W.M., 1977. Flow of weak rocks in the Appalachian Plateau folds. American Association of Petroleum Geologists Bulletin 61, 653–670.

Zapata, T.R., Allmendinger, R.W., 1996. Growth stratal records of instantaneous and progressive limb rotation in the Precordillera thrust belt and Bermejo basin, Argentina. Tectonics 15, 1065–1083.